Available online at www.sciencedirect.com
SCIENCE DIRECT®
International Journal of Heat and Mass Transfer 48 (2005) 243–253
International Journal of HEAT and MASS TRANSFER
www.elsevier.com/locate/ijhmt

An experimental study of heat transfer in oscillating flow through a channel filled with an aluminum foam

K.C. Leong *, L.W. Jin

School of Mechanical and Production Engineering, Nanyang Technological University, 50 Nanyang Avenue, Singapore 639798, Singapore

Received 13 May 2004; received in revised form 23 August 2004

Abstract

An experimental study has been conducted on the heat transfer of oscillating flow through a channel filled with aluminum foam subjected to a constant wall heat flux. The surface temperature distribution on the wall, velocity of flow through porous channel and pressure drop across the test section were measured. The characteristics of pressure drop, the effects of the dimensionless amplitude of displacement and dimensionless frequency of oscillating flow on heat transfer in porous channel were analyzed. The results revealed that the heat transfer in oscillating flow is significantly enhanced by employing porous media in a plate channel. The cycle-averaged local Nusselt number increases with both the kinetic Reynolds number Re_ω and the dimensionless amplitude of flow displacement A_0. The length-averaged Nusselt number is effectively increased by increasing the kinetic Reynolds number from 178 to 874 for $A_0 = 3.1$–4.1. Based on the experimental data, a correlation equation of the length-averaged Nusselt number with the dimensionless parameters of Re_ω and A_0 is obtained for a porous channel with $L/D_h = 3$.
© 2004 Elsevier Ltd. All rights reserved.

Keywords: Oscillating flow; Oscillatory frequency; Maximum displacement; Porous channel; Nusselt number; Heat transfer

1. Introduction

The recent acceleration in chip power dissipation and thermal requirements has placed thermal design on a critical path in the development process of almost all kinds of electronic components. The need for higher performance and an increased level of functional integration as well as die size optimization on the device leads to preferential clustering of higher power units on the electronic packages. Currently, typical desktop and mobile processor peak power consumptions are about 100 and 30 W [1], respectively. Under conventional natural or forced convection cooling techniques, the most common method is to increase the air flow rate and solid-air contact surface area. These methods, however, will increase the backpressure and the acoustic noise, while increasing the volume of heat sink at the same time. Conventional heat sinks are not capable of removing such a high heat flux with an appropriate volume for maintaining a proper operational temperature in modem electronic devices. The porous medium has emerged as an effective method of heat transfer enhancement, due to its large surface area to volume ratio and intense mixing of fluid flow.

Rachedi and Chikh [2] investigated the enhancement of electronic cooling by attachment of porous materials

* Corresponding author. Tel.: +65 6790 5596; fax: +65 6792 2619.
E-mail address: mkcleong@ntu.edu.sg (K.C. Leong).

0017-9310/$ - see front matter © 2004 Elsevier Ltd. All rights reserved.
doi:10.1016/j.ijheatmasstransfer.2004.08.025

Nomenclature

A_{heated}	heated area
A_0	dimensionless maximum flow displacement, $(x_{\max}/D_{\text{h}})$
D_{h}	hydraulic diameter of the channel, $(5H/3)$
D_{i}	inside diameter of the pipe
d_{l}	ligament diameter of porous media
f	oscillatory frequency
$f_{\max}$	maximum friction factor defined in Eq. (3)
H	height of the channel
h_x	local heat transfer coefficient defined in Eq. (6)
K	permeability of the porous medium
k_{f}	thermal conductivity of fluid
L	length of the test section
Nu_x	cycle-averaged local Nusselt number
$Nu_{\text{l-avg}}$	length-averaged Nusselt number
$Nu_{\text{s-avg}}$	space-cycle averaged Nusselt number defined in Eq. (9)
ΔP	pressure drop across the test section
$\Delta P_{\max}$	maximum pressure drop across the test section
Q	power input
q''	heat flux
R_k	thermal conductivity ratio
Re_{ω}	kinetic Reynolds number defined in Eq. (2)
$Re_{\text{l-max}}$	maximum ligament Reynolds number defined in Eq. (4)
T_{w}	cycle-averaged local surface temperature
T_{i}	cycle-averaged temperature at the inlet of test section
$\overline{T}_{\text{w}}$	space-cycle averaged wall temperature
$\overline{T}_{\text{m}}$	space-cycle averaged temperature of the fluid at mixing chamber
$U_{\max}$	maximum velocity of fluid in porous media
w	channel width
$x_{\max}$	amplitude of flow displacement

Greek symbols

ω	angular frequency
ν_{f}	kinematic viscosity of fluid
ρ	density of fluid
δ	uncertainty
ε	porosity of the porous medium

above the electronic components. Their results indicate that for porous media with moderate thermal conductivity ($2 < R_k < 10$) the decrease in the maximum temperature is about 15% and substantial cooling enhancement is obtained with materials of high thermal conductivity. Bhattacharya and Mahajan [3] experimentally studied forced convective heat transfer in novel finned metal foam heat sinks for application in electronic cooling. Experiments were conducted on aluminum foams of 90% porosity and pore density corresponding to 5 and 20 PPI, where PPI stands for pores per inch. Their results show that heat transfer was significantly enhanced when fins were incorporated in metal foams, and the heat transfer coefficient increased with an increase in the number of fins until the addition of more fins retarded heat transfer due to interference of thermal boundary layers. Thermal performance of the aluminum-foam heat sinks can significantly increase heat removal from high-density electronic devices [4]. With only about 25% of the mass of a conventional parallel-plate heat sink, an aluminum foam heat sink has a thermal resistance which is 28% lower than conventional parallel-plate heat sinks. Therefore, the porous metal foam heat sink may satisfy the needs for compact cooling system.

However, one-directional flow through the porous channel yields a relatively high temperature difference along the flow direction on the substrate surface. Hwang and Chao [5] studied the heat transfer of sintered bronze bead channels with uniform heat fluxes of up to 3.2 W/cm^2. They observed a local surface temperature difference of more than 50 °C between the most upstream and the most downstream locations in the case of $q'' = 3.2\,\text{W/cm}^2$ in their experiments. For modern high-speed microprocessors, the reliability of transistors and operating speed are not only influenced by the average temperature but also by temperature uniformity on the substrate surface. With increasing performance, the non-uniformity of on-die power distribution increases, and there are regions of the die with high heat flux densities. The temperature of the hot spot can often affect calculated performance due to prolonged gate delay, and will always govern the overall reliability of the silicon. Therefore, maintaining the uniformity of on-die temperature distribution below certain limits is imperative in thermal design [6]. It is conceivable that oscillating flow will produce a more uniform temperature distribution on a substrate surface due to the two thermal entrance regions of oscillating flow.

The works related to heat transfer enhancement in an oscillating flow through an empty channel tube have been conducted analytically and experimentally in the past two decades [7–9]. Recently, Walsh et al. [10] experimentally investigated forced convection cooling in micro-electronic cabinets by oscillatory flow techniques. Their results show that electronic component operating temperatures can be reduced by as much as 40% when an oscillatory flow device is employed. Zhao and Cheng

[11] presented both experimental and numerical results for laminar forced convection of an incompressible periodically reversing flow in a pipe of finite length at constant heat flux. The averaged heat transfer rate was found to increase with both the kinetic Reynolds number and the dimensionless oscillation amplitude but decrease with the length-to-diameter ratio.

Compared to the foregoing research works that were performed on oscillating flow through empty channels, published investigations on oscillating flow heat transfer through porous channels are really scarce. Khodadadi [12] treated analytically the problem of oscillating flow through a porous medium channel bounded by two impermeable parallel plates with the assumption of negligible inertia effects. His results showed that the oscillatory fully developed flow in porous media is dependent on the porous medium shape parameter and Stokes number. Sozen and Vafai [13] conducted a numerical study of compressible flow through a packed bed. The effect of oscillating boundary conditions on the transport phenomena was investigated with the packed wall insulated. More recently, Fu et al. [14] and Leong and Jin [15] reported the results for heat transfer in porous channels in oscillating flow with reticulated vitreous carbon and metal foam materials. They reported that the length-averaged Nusselt number for oscillating flow is higher than that for steady flow. The effects of thermal conductivity and permeability of different metal foam materials on heat transfer were analyzed. However, the effects of the kinetic Reynolds number Re_ω and the dimensionless amplitude of flow displacement A_0 on heat transfer of oscillating flow in porous channel have not been discussed. The present work is an extension of the authors' previous studies in heat transfer of porous media.

In this paper, the heat transfer of the oscillating flow through a channel filled with an aluminum foam subjected to a constant wall heat flux was experimentally investigated. The characteristics of oscillating flow in porous channel, the effects of displacement and frequency on heat transfer in oscillating flow through the porous channel were analyzed. Based on the experimental data, a correlation equation of the length-averaged Nusselt number with the dimensionless parameters of Re_ω and A_0 is obtained for a porous channel with $L/D_h = 3$. The correlation equation will be useful when employing oscillating flow through a porous channel in electronics cooling.

2. Experimental setup and procedures

2.1. Experimental facility

A schematic diagram of the experimental setup is depicted in Fig. 1. The facility consists of four major parts: oscillating flow generator, test section, coolers and unheated sections and velocity measurement section. The oscillating flow generator is a mechanism that generates a sinusoidal oscillating flow. The mechanism consists of a compression cylinder, a piston and a crankshaft with adjustable stroke lengths. These were firmly fixed at the base onto a solid board by screw bolts to withstand strong vibrations caused by the oscillating motion of the generator. The supporting shafts are two ball bearings elevated to the height of the piston axis to ensure smooth oscillatory movement. The crankshaft was driven by a DC electric motor (LEESON 0.75 kW) with variable speed capabilities to drive the piston forward and backward sinusoidally. By adjusting the motor speed through a transducer, oscillating flows with different frequencies were generated. In the present experiments, oscillating frequencies from 1 to 10 Hz were employed. Different oscillating amplitudes were obtained by varying the distance of the crank from the plate center. The locations of 26, 30 and 34 mm from the center of the plate were selected and the oscillating flows with the maximum displacement of 52, 60 and 68 mm were provided.

Fig. 2 shows the cross sectional view of the test section and the structure of aluminum foam 40 PPI. As shown in Fig. 2(a), the test section is a well-shaped block of aluminum foam 40 PPI with dimensions of $50 \times 50 \times 10$ mm. It was made by the sintering technique. The typical structure of sintered metal foam is shown in Fig. 2(b). The pores inside the porous media are open to others and fully interconnected. Solid ligaments form the reticulated structure in the metal foam. The metal foam possesses a large surface area to volume ratio and a high permeability. The ligament diameter d_l of 0.114 mm was measured for aluminum 40 PPI using a Scanning Electron Microscope. The fully opened pore structure provides a relatively low flow restriction. A film heater ($60\,mm \times 60\,mm \times 10\,mm$) was firmly mounted on the bottom of channel to supply a constant heat flux, and a 1-mm copper plate with eight narrow slots perpendicular to the flow direction was attached on the surface of film heater. To distribute the heat evenly on the copper plate and to reduce gap thermal resistance, thermal grease was used as a filling material between the heater and the copper plate. A small hole in the Teflon material was used to allow the insertion of 10 thermocouples into the heated section. The copper plate was cleaned and eight thermocouples (K-type) were fixed into eight narrow slots. The locations of these thermocouples X/D_h (where $D_h = 5H/3$ is the hydraulic diameter of the channel) are 0, 0.4284, 0.8568, 1.2858, 1.7142, 2.1456, 2.5716 and 3. The other two thermocouples were placed at the inlet and outlet to measure the bulk temperatures. The two taps of the pressure transducer (VALIDYNE DP15) are located before and after the test section for pressure drop measurements. By adjusting the supply voltage to the heater, which could

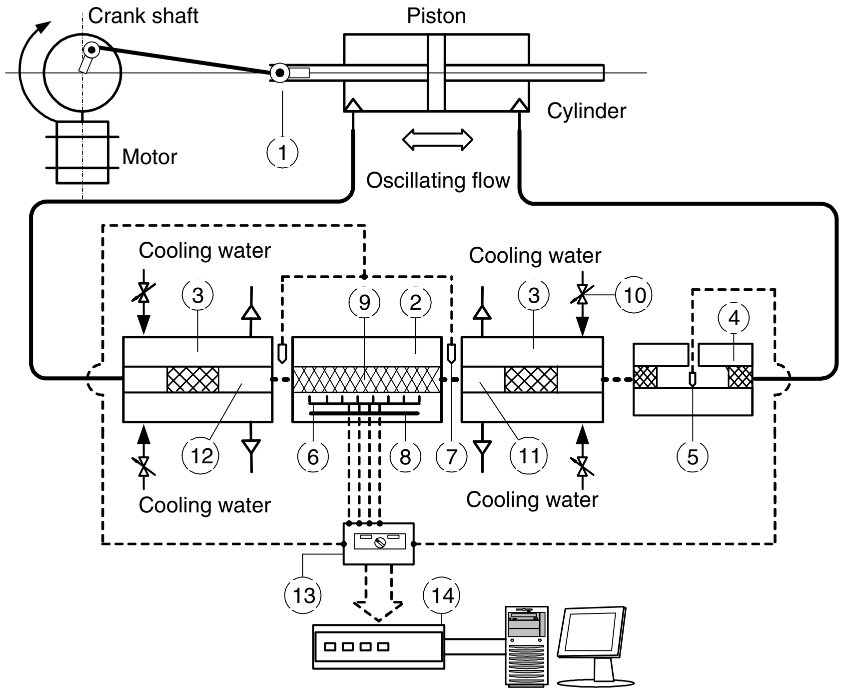

Fig. 1. Schematic diagram of experimental system: (1) oscillating flow generator, (2) test section, (3) coolers and unheated section, (4) velocity measurement section, (5) hot-wire probe, (6) thermocouples, (7) pressure transducer, (8) film heater, (9) porous metal foam, (10) valve, (11) inlet bulk, (12) outlet bulk, (13) voltage amplifier and (14) data acquisition and computer system.

be monitored through the display from a digital voltmeter and an ammeter, the desired input heat flux could be obtained. In present experimental study, input power ranged from 20 to 60 W. The whole test section was made of Teflon material and the channel was well insulated.

The two unheated sections were formed by two blocks of aluminum 10 PPI foam as shown in Fig. 1. They were installed adjacent to the two ends of the test section. The aluminum foam in unheated sections was used to build up a uniform velocity profile for flow through the test section. Two pairs of the coolers were installed at the upper and bottom of the two unheated sections. The heat carried by the flow was transferred to the surface of coolers through the unheated porous material. The velocity measurement section was made of an aluminum column with diameter of 16 mm. A hot-wire sensor (TSI 1210-20w) was mounted at the center of the two ends packed with 40 mesh woven screen discs. The packed screen provides a uniform velocity profile, so that the measured velocity is the cross-section averaged velocity through the test section.

2.2. Experimental procedures and data reduction

Before the commencement of the experiments, all thermocouples, pressure sensors and hot-wire were carefully calibrated. By looping the test section to the oscillating flow regenerator, heat transfer experiments of oscillating flow can be conducted. Cooling water with room temperature was forced through the four coolers installed to cooling the dissipated heat. The frequencies of oscillating flow were adjusted by controlling the motor speed. For fixed amplitude, the experiments were carried out by increasing the oscillating frequency while keeping the power input unchanged. To obtain a cyclic steady state, the temperatures on the substrate surface were monitored by the data acquisition system. 100 cycles of data were obtained under different sampling rates by adjusting the acquired A/D rate for different oscillating frequency. When a set of reading had been recorded, the test apparatus had to be cooled down to temperature of ambient about 25 °C before the next set of experiments can be started. In the present experiments, the flow velocity through the test section, the pressure drop across the test section and the temperature distribution along the axial direction on the substrate surface were measured. All the signals were collected by a data acquisition system consisting of a voltage amplifier (KEITHLEY MB40), a 12-bit A/D card (KEITHLEY DAS-1402), control software (CEC TestPoint) and a computer.

For electronic cooling applications, time-averaged characteristics are of practical interest instead of instan-

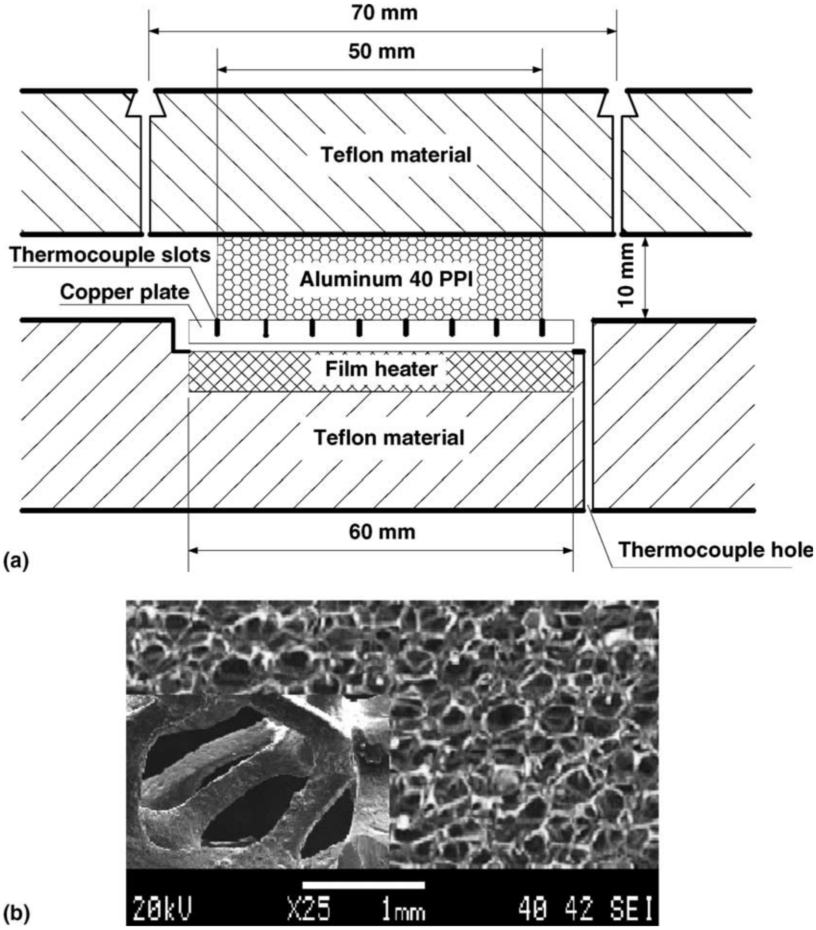

Fig. 2. Test section: (a) Cross sectional view of test section and (b) aluminum foam 40 PPI.

taneous quantities. As mentioned earlier, instantaneous higher power dispersion may not damage the electronics components, but a long-lasting higher temperature will decrease their performance or even destroy them. Therefore, to minimize the data reduction uncertainty, the cycle-averaged method was employed to reduce the present experimental data over 100 complete cycles. The heat losses through the insulation were measured at different surface temperatures under the condition of no airflow through the test section. The net heat inputs were obtained by subtracting the heat losses from gross heat inputs at the corresponding temperature. By calculating the air enthalpy rise along the test section, the error of energy balance was found to be within 6%. The uncertainties of the measured data can be classified into two groups: random uncertainties, which can be treated statistically; and systematic uncertainties, which cannot be treated in the same way. With careful experimentation, systematic uncertainty can be minimized. The accuracies of the thermocouple temperature and pressure transducer readings are within ±0.1 °C and ±0.25% of full-scale, respectively. The accuracy of the velocity measured by the hot-wire anemometer is ±0.01 m/s. After the cycle-averaging process, uncertainties of temperature, velocity and pressure are 3.0%, 2.0% and 2.0%, respectively. The uncertainties of f, D_h, A_0, d_l and Q are estimated to be 2.5, 1.0, 1.0, 2.0 and 3.0, respectively. The uncertainties of Re_ω and Nu_x were determined by the method described by Taylor [16]. If $v, \ldots, y, \ldots, z$ are measured quantities with uncertainties $\delta v, \ldots, \delta y, \ldots, \delta z$, and the measured values are used to compute the function $q(v, \ldots, y, \ldots, z)$, then the uncertainty in q is

$$\delta q = \sqrt{\left(\frac{\partial q}{\partial v}\delta v\right)^2 + \cdots + \left(\frac{\partial q}{\partial y}\delta y\right)^2 + \cdots + \left(\frac{\partial q}{\partial z}\delta z\right)^2} \tag{1}$$

In the present experiments, the uncertainties of the measured data were assumed to be independent and random with normal distribution. Using Eq. (1), the uncertainties of Re_ω, and Nu_x are calculated to be 3.9% and 5.7%, respectively.

3. Results and discussions

3.1. Characteristics of oscillating flow through porous channel

Fig. 3(a) shows a typical variation of flow velocity and pressure drop through the test section along the cycles of oscillating flow with the maximum flow displacement $x_{\max} = 60$ mm for oscillating flow. The results were obtained under the unheated condition with the same test configuration. It can be seen that the profiles of pressure drop and flow velocity increase with the increase of oscillatory frequency, and vary almost sinusoidally due to the reversing flow direction. High pressure drop corresponds to high flow velocity which shows that the phase difference between the velocity and pressure is very small for this type of porous media. Khodadadi [12] showed that the phase lag θ_n between the velocity component and the pressure gradient can be predicted using the equation, $\theta_n = \tan^{-1}(n\alpha^2/\gamma^2)$ where $\alpha = (w^2\omega/\nu_f)^{1/2}$ is the Stokes number and $\gamma = (w^2\varepsilon/K)^{1/2}$ is the shape parameter of porous medium. For the present experiments, kinematic viscosity ν_f of the air is taken to be $15.66 \times 10^{-6}\,\mathrm{m^2/s}$, porosity ε and permeability K of aluminum 40 PPI are about 0.9 and $3 \times 10^{-8}\,\mathrm{m}^2$, respectively. The phase lag θ_n is calculated to be 3° for the case presented in Fig. 3(a) in which the angular frequency $\omega = 27$ rad/s and cycle number $n = 1$. This indicates that the phase difference between velocity and pressure drop is very small and the trends observed in our experiments are in agreement with the analytic relation of Khodadadi [12]. From this figure, it is noted that maximum pressure drop across the channel filled with aluminum 40 PPI foam is lower than 300 Pa for an oscillatory frequency of 6.6 Hz. This implies that the required power for driving the oscillating flow through the test section is not high. A similar result was obtained by Fu et al. [14]. Fig. 3(b) presents the variation of pressure drop and velocity versus periods for different flow displacements with the same oscillatory frequency. The profiles of flow velocity and pressure drop across the test section increase with the increase of the maximum oscillation displacement. Once again, the pressure drop varies in the same measure as velocity for different displacements of flow movement.

Fig. 4 presents the maximum pressure drop versus kinetic Reynolds number for maximum displacement $x_{\max} = 52$, 60 and 68 mm in oscillating flow. The definition of kinetic Reynolds number is based on the oscillatory frequency f and is defined as

$$Re_\omega = \frac{2\pi f D_h^2}{\nu_f} \tag{2}$$

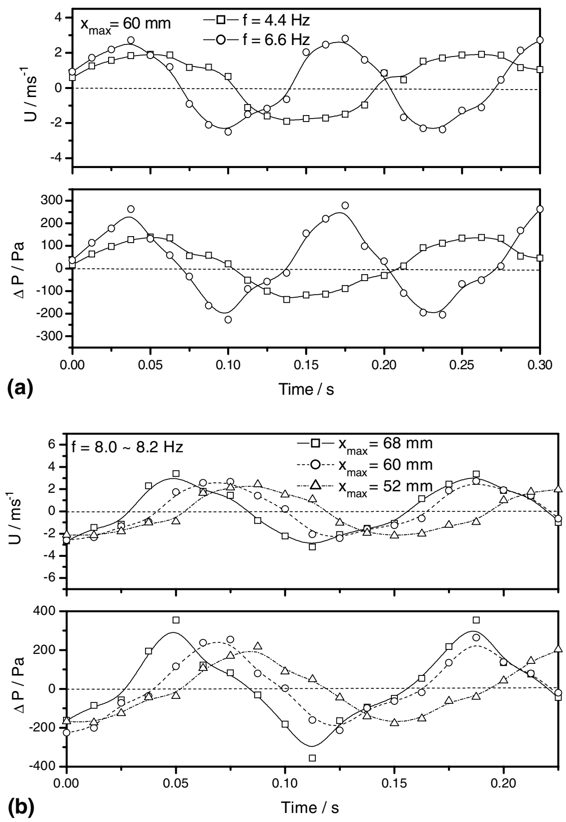

Fig. 3. Characteristics of oscillating flow through a porous channel: (a) variations of pressure drop and velocity of different f for $x_{\max} = 60$ mm and (b) variations of pressure drop and velocity of different $x_{\max}$ for $f = 8.0$–8.2 Hz.

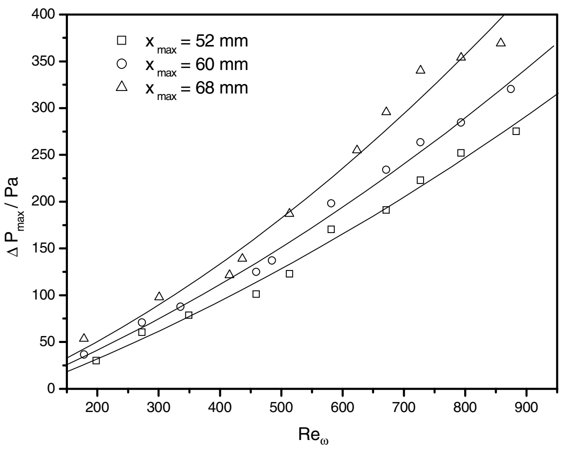

Fig. 4. Maximum pressure drop versus kinetic Reynolds number for $x_{\max} = 52$–68.

where $D_h = 5H/3$ and ν_f are the hydraulic diameter of channel and kinematic viscosity of the fluid, respectively. It is shown that higher maximum displacement reaches higher maximum pressure drop with the same kinetic Reynolds number in oscillating flow. The difference between maximum pressure drop for various displacements increases with an increase in the kinetic Reynolds number. This implies that the ratio of the maximum pressure drop to kinetic Reynolds number for flow with high displacement is larger than that of flow with low displacement. For different maximum displacements, the maximum pressure drop increases rapidly with an increase in the kinetic Reynolds number, i.e. oscillatory frequency.

The maximum friction factor of oscillating flow through the channel filled with aluminum foam was calculated by the maximum pressure drop factor and maximum Reynolds number. The dimensionless amplitude of flow displacement A_0 is defined as x_{max}/D_h. Eqs. (3) and (4) are employed in the calculations.

$$f_{max} = \frac{\Delta P_{max} D_h}{\frac{1}{2}\rho (U_{max})^2 L} \tag{3}$$

where ΔP_{max} and U_{max} are the maximum pressure drop and maximum cross-sectional flow velocity in one cycle of oscillating flow, respectively. ρ is the density of the fluid, and L is the length of the test section.

$$Re_{l\text{-}max} = \frac{U_{max} d_l}{\nu_f} \tag{4}$$

where d_l is the ligament diameter of porous media. The definition of the maximum Reynolds number $Re_{l\text{-}max}$ in Eq. (4) is based on the ligament diameter of aluminum foam. As shown in Fig. 5, the maximum friction factor for different dimensionless amplitude of displacement decreases asymptotically with the maximum ligament Reynolds number increase. The same trend of maximum pressure drop factor versus Reynolds number based on the hydraulic diameter was obtained by Zhao and Cheng [17] for oscillatory flow through a pipe filled with a woven screen.

3.2. Heat transfer of oscillating flow in porous and empty channels

Fig. 6 compares the pressure drops of oscillating flow in the porous channel and an empty channel for different maximum displacement flows. The result was obtained under unheated condition in the same test section. It is obvious that the pressure drop profile in the channel filled with aluminum 40 PPI foam is much higher than that in the empty channel for varying flow amplitudes. It is noted that the maximum pressure drop increases with the increase of flow displacement in porous channel, but it is inconspicuous in the empty channel.

Fig. 7(a) presents the cycle-averaged temperature distribution on the substrate surface along the axial direction in oscillating flow with oscillatory frequency $f = 3.1$–3.8 Hz and power input $Q = 20$, 40 and 60 W for both empty and porous channels. For both empty and porous channels, there are two thermal entrance regions in the test section due to the reversing flow direction. The surface temperatures located at the two entrances are lower than that at the center of the test section. The local surface temperature distribution curves are convex with the maximum point at the center of the test section. It is obvious that for different input power, the surface temperature profile in the empty channel is much higher than that in channel filled with metal foam. The advantages of large surface-area-to-volume ratio and intense mixing of flowing flow of metal foam resulted in a much lower surface temperature

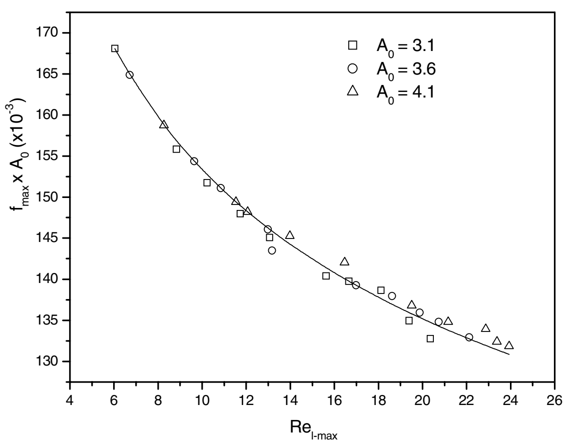

Fig. 5. Maximum friction factor versus the maximum ligament Reynolds number for $A_0 = 3.1$–4.1.

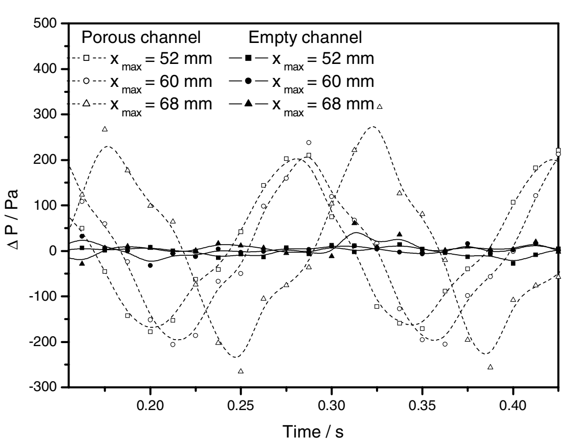

Fig. 6. Comparison of variations of pressure drop in porous and empty channels.

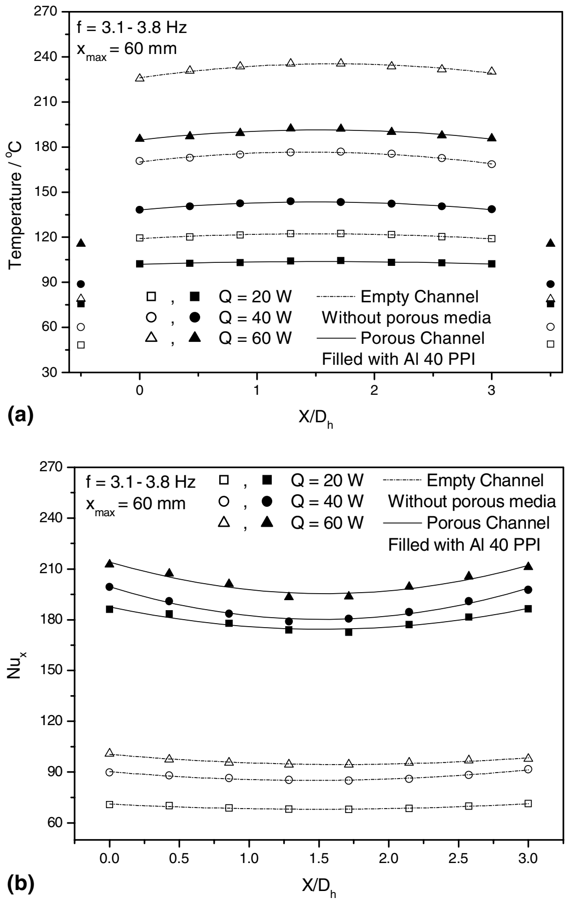

Fig. 7. Comparison of heat transfer in oscillating flow through porous and empty channel: (a) cycle-averaged surface temperature distribution and (b) cycle-averaged local Nusselt number distribution.

distribution in a porous channel subjected to oscillating flow.

Fig. 7(b) shows the cycle-averaged local Nusselt number in both empty and porous channels along the dimensionless axial distance with the range of oscillation frequency from 3.1 to 3.8 Hz for power input $Q = 20$, 40 and 60 W. The cycle-averaged local Nusselt number was calculated by

$$h_x = \frac{Q}{A_{\text{heated}}(T_w - T_i)} \tag{5}$$

$$Nu_x = \frac{h_x D_h}{k_f} \tag{6}$$

where Q is the power input and A_{heated} is the heated area, h_x, T_w and T_i are the heat transfer coefficient, the local wall temperature and the bulk air inlet temperature, respectively. $D_h = H/3$ is the hydraulic diameter of porous channel, where H is the channel height. From Fig. 7(b), it can be seen that the cycle-averaged local Nusselt number decreases as dimensionless location X/D_h approaches the center of the test section. The Nusselt number distribution curves are concave with the minimum value around the center of the test section as symmetric point. The results obtained by Fu et al. [14] and Zhao and Cheng [11] show the same trends of Nusselt number distribution for oscillating flow in a porous channel and an empty tube, respectively. It is obvious that the cycle-averaged Nusselt number for oscillating flow in porous channel is much higher than that in an empty channel, due to the inserted aluminum foam. For the case of power input $Q = 60$ W and frequency $f = 3.1$–3.8 Hz, the length-averaged Nusselt number (the averaged value of the cycle-averaged local Nusselt number along the axial direction) of oscillating flow in the porous channel is about 2.3 times than that of an empty channel. It is noted that the difference of cycle-averaged local Nusselt number between the two ends of the test section and center locations in porous channel is larger than that in empty channel. It indicates that heat transfer performance can be significantly enhanced at the thermal entrance region in oscillating flow through a channel filled with sintered metal foam.

3.3. Effects of frequency and displacement of oscillating flow on the heat transfer

The effect of kinetic Reynolds number ($Re_\omega = 2\pi f D_h^2/\nu_f$, i.e. dimensionless oscillatory frequency) on the cycle-averaged local surface temperature for amplitudes of flow displacement $x_{max} = 68$ and 52 mm with the power input $Q = 40$ W is presented in Fig. 8(a). It can be observed that the cycle-averaged local surface temperature profile decreases with the increase of the kinetic Reynolds number for different flow displacement. It implies that high oscillatory frequency corresponds to low cycle-averaged local surface temperature. Once again, it is seen that the temperature distribution curves are of convex shape with the maximum point located around the center of the test section. Fig. 8(b) shows the effect of kinetic Reynolds number on the cycle-averaged local Nusselt number of oscillating flow in porous channel for $x_{max} = 68$ and 52 mm. It is shown that the cycle-averaged local Nusselt number increases with the increase of kinetic Reynolds number. It is also seen that for varying oscillatory frequency, the distribution curves of cycle-averaged local Nusselt number are concave with the center of the test section as the symmetric point.

Fig. 9 shows the effect of dimensionless amplitude of flow displacement A_0 on heat transfer of oscillating flow in a porous channel with different kinetic Reynolds numbers. It can be seen from Fig. 9(a) that the temperature profile decreases with an increase in the dimensionless amplitude of flow displacement for various kinetic

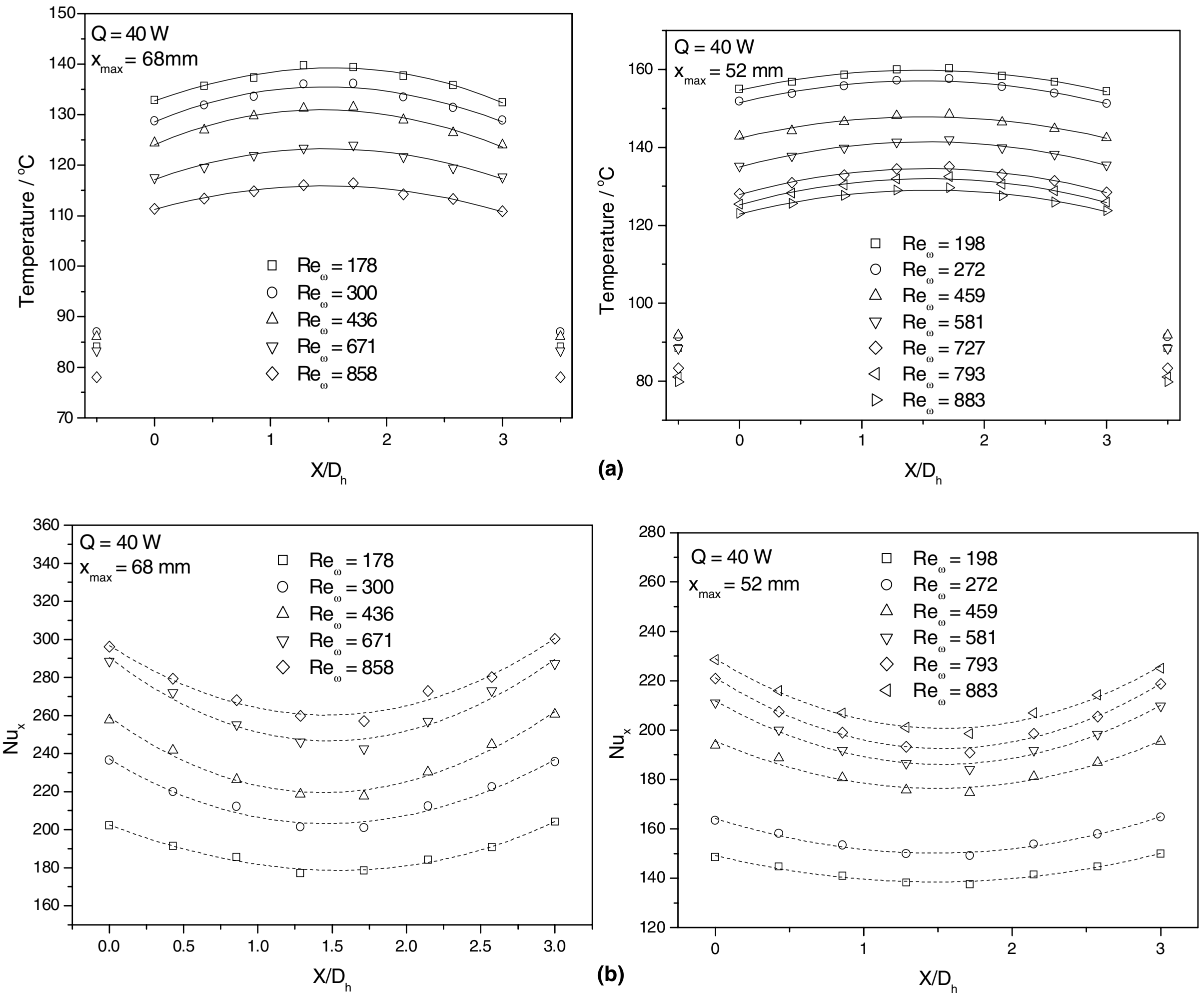

Fig. 8. Effect of kinetic Reynolds number on heat transfer of oscillating flow in a porous channel: (a) distribution of cycle-averaged surface temperature and (b) distribution of cycle-averaged local Nusselt number.

Reynolds numbers. For different displacements, the same shape of temperature distribution curve was obtained as in Fig. 8(a). Fig. 9(b) presents the effect of dimensionless parameter A_0 on the distribution of cycle-averaged Nusselt number at different Reynolds numbers. It is clear that the profile of cycle-averaged local Nusselt number for large A_0 is higher than that for small A_0. A closer observation shows that the curvature of Nusselt number distribution curves for large displacements is larger than those for small displacements. This implies that length of the thermal entrance region for oscillating flow with large amplitude of displacement is longer than that for oscillating flow with small amplitude of displacement. It can be deduced that higher heat transfer rates can be obtained by larger displacement oscillating flows with high kinetic Reynolds number in a porous channel.

In order to evaluate the effects of dimensionless amplitude of flow displacement A_0 and kinetic Reynolds number Re_ω on the total heat dissipation rate in a porous channel subjected to oscillating flow, the length-averaged Nusselt number was used to calculate the averaged Nusselt number of the whole length of the section. Fig. 10 presents the length-averaged Nusselt number versus kinetic Reynolds number with different dimensionless amplitude of flow displacement for a porous channel with $L/D_h = 3$. Generally, the length-averaged Nusselt number $Nu_{\text{l-avg}}$ increases with both dimensionless parameters of A_0 and Re_ω. An interesting finding in this figure is that for a fixed dimensionless amplitude of flow displacement A_0 the length-averaged Nusselt number approaches a constant value for a kinetic Reynolds number Re_ω of about 874. This implies that very high oscillatory frequency has very little contribution to an

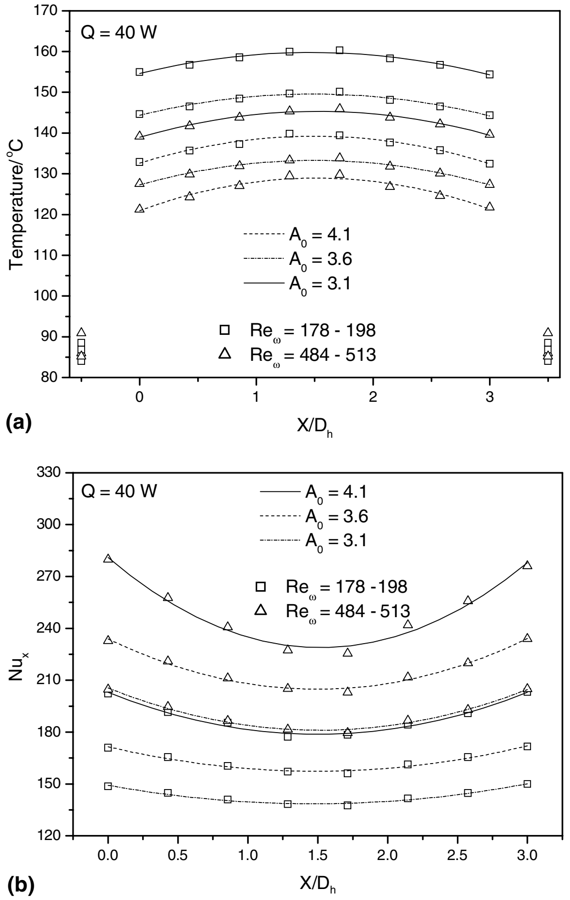

Fig. 9. Effect of dimensionless amplitude of flow displacement on heat transfer of oscillating flow in a porous channel: (a) distribution of cycle-averaged surface temperature and (b) distribution of cycle-averaged local Nusselt number.

increase in heat transfer rate in oscillating flow through a porous channel. This suggests that oscillating flow at relatively low frequency and high amplitude of displacement has a substantial effect on the heat transfer behavior in a porous channel since the temperature fluctuation on the wall surface cannot follow the oscillatory velocity at a very high frequency. The length-averaged Nusselt number is effectively increased by increasing the kinetic Reynolds number in a suitable range from 178 to 874 for $L/D_h = 3$ and $A_0 = 3.1$–4.1.

Using the least squares method, the data in Fig. 10 can be collapsed to a fitting line as shown in Fig. 11. The resulting correlation equation of the length-averaged Nusselt number with the dimensionless amplitude of flow displacement and kinetic Reynolds number for oscillating flow with $Re_\omega = 150$–900 and $A_0 = 3.1$–4.1 in a porous channel of $L/D_h = 3$ is

$$Nu_{\text{l-avg}} = 12.38 A_0^{0.95} Re_\omega^{0.31} \tag{7}$$

Eq. (7) indicates that the effect of A_0 on the heat transfer behavior in oscillating flow is more dominant than that of Re_ω due to the larger exponent of A_0. It implies that higher heat transfer performance can be obtained by oscillating flow through a porous channel with relatively low frequency and high displacement. A similar correlation equation obtained by Zhao and Cheng [11] is given by

$$Nu_{\text{s-avg}} = 0.02 A_0^{0.85} Re_\omega^{0.583} \tag{8}$$

Here, $Nu_{\text{s-avg}}$ is the space-cycle averaged Nusselt number defined as

$$Nu_{\text{s-avg}} = q'' D_i / k_f (\overline{T}_w - \overline{T}_m) \tag{9}$$

where $\overline{T}_w, \overline{T}_m$ and D_i are the space-cycle averaged wall temperature, space-cycle averaged temperature at the mixing chamber and the diameter of the pipe, respec-

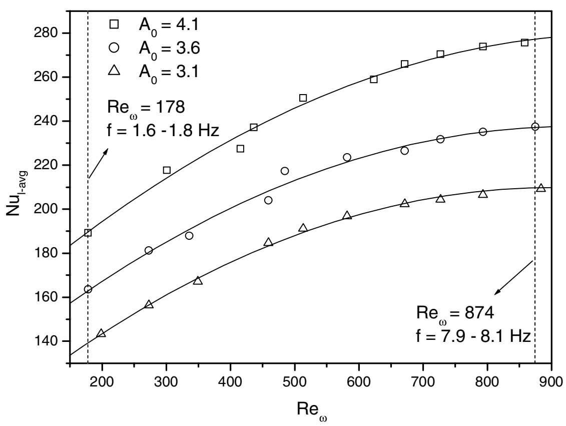

Fig. 10. Effects of A_0 and Re_ω on the length-averaged local Nusselt number for a porous channel with $L/D_h = 3$.

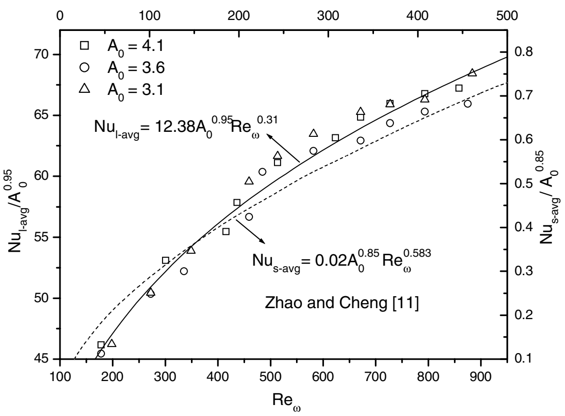

Fig. 11. Correlation equation of the length-averaged local Nusselt number with A_0 and Re_ω for a porous channel with $L/D_h = 3$.

tively. Eq. (8) gives the space-cycle Nusselt number in terms of Re_ω and A_0 in a long empty tube with constant heat flux subjected to oscillatory flow. The high heat transfer rate of oscillating flow through porous media obtained by the present study and the different definitions of the averaged Nusselt number result in the large difference in the constants of Eqs. (7) and (8).

4. Conclusions

In the present study, the heat transfer enhancement of oscillating flow through a channel filled with aluminum foam was experimentally investigated. The flow velocity, pressure drop across the section and the surface temperature were measured. The characteristics of oscillating flow in porous channel, the effects of displacement and frequency on heat transfer in oscillating flow through the porous channel were analyzed. The following conclusions can be drawn from this study:

(1) The maximum pressure drop of oscillating flow in a porous channel increases with the kinetic Reynolds number Re_ω and with the dimensionless amplitude of flow displacement A_0.
(2) The cycle-averaged local surface temperatures in a porous channel subjected to oscillating flow are much lower than that in an empty channel. The length-averaged local Nusselt number for oscillating flow in porous channel can be up to several times larger than that in empty channel.
(3) The heat transfer enhancement of oscillating flow through a porous channel increases with the dimensionless amplitude of flow displacement and with oscillatory frequency in a suitable range. The increase of cycle-averaged local Nusselt number will be reduced if kinetic Reynolds number is very high. In the present experiments, the favorable range of kinetic Reynolds number for enhancing heat transfer is from 178 to 874.
(4) Based on the present experimental study, a correlation equation of length-averaged Nusselt number with the dimensionless parameters of Re_ω and A_0 is obtained for a porous channel with $L/D_h = 3$. Heat transfer enhancement depends more sensitively on flow displacement than on oscillatory frequency. This correlation equation will be useful to determine heat transfer rates in oscillating flow through a porous channel for applications in electronics cooling.

References

[1] S. Gochman, R. Ronen, I. Anati, A. Berkovits, T. Kurts, A. Naveh, A. Saeed, Z. Sperber, R.C. Valentine, The Intel Pentium M processor: microarchitecture and performance, Intel Technol. J. 7 (2003) 21–36.

[2] R. Rachedi, S. Chikh, Enhancement of electronic cooling by insertion of foam materials, Heat Mass Transf. 37 (2001) 371–378.

[3] A. Bhattacharya, R.L. Mahajan, Finned metal foam heat sinks for electronics cooling in forced convection, J. Electron. Packag. 124 (2002) 155–163.

[4] S.Y. Kim, J.W. Paek, B.H. Kang, Thermal performance of aluminum-foam heat sinks by forced air cooling, IEEE Trans. Compon. Packag. Tech. 26 (2003) 262–267.

[5] G. Hwang, C. Chao, Heat transfer measurement and analysis for sintered porous channels, ASME J. Heat Transf. 116 (1994) 456–464.

[6] R.L. Mahajan, R. Nair, V. Wakharkar, J. Swan, J. Tang, G. Vandentop, Emerging directions for packaging technologies, Intel Technol. J. 06 (2002) 62–75.

[7] U.H. Kurzweg, Enhanced heat conduction in oscillating viscous flows within parallel-plate channels, J. Fluid Mech. 156 (1985) 291–300.

[8] D. Gedeon, Mean-parameter modeling of oscillating flow, ASME J. Heat Transf. 107 (1986) 513–518.

[9] R. Siegel, Influence of oscillation-induced diffusion on heat transfer in a uniformly heated channel, ASME J. Heat Transf. 109 (1987) 244–247.

[10] T.E. Walsh, K.T. Yang, V.W. Nee, Q.D. Liao, Forced convection cooling in microelectronic cabinets via oscillatory flow techniques, Experiment. Heat Transf., Fluid Mech. Thermodyn. 2 (1993) 1846–1853.

[11] T.S. Zhao, P. Cheng, Oscillatory heat transfer in a pipe subjected to a laminar reciprocating flow, ASME J. Heat Transf. 118 (1996) 592–598.

[12] J.M. Khodadadi, Oscillatory fluid flow through a porous medium channel bounded by two impermeable parallel plates, J. Fluids Eng. 113 (1991) 509–511.

[13] M. Sozen, K. Vafai, Analysis of oscillating compressible flow through a packed bed, Int. J. Heat Fluid Flow 12 (1991) 130–136.

[14] H.L. Fu, K.C. Leong, X.Y. Huang, C.Y. Liu, An experimental study of heat transfer of a porous channel subjected to oscillating flow, ASME J. Heat Transf. 123 (2001) 162–170.

[15] K.C. Leong, L.W. Jin, Heat transfer of oscillating flow and steady flows in a channel filled with porous media, Int. Comm. Heat Mass Transf. 31 (2004) 63–72.

[16] J.R. Taylor, An Introduction to Error Analysis—Study of Uncertainty in Physical Measurements, Oxford University Press, 1995.

[17] T.S. Zhao, P. Cheng, Oscillatory pressure drop through a woven-screen packed column subjected to a cyclic flow, Cryogenics 36 (1996) 333–341.